Comparing antithetic trends of data for the pion-photon transition form factor

A. P. Bakulev,[1,*] S. V. Mikhailov,[1,†] A. V. Pimikov,[1,2,‡] and N. G. Stefanis[3,§]

[1]*Bogoliubov Laboratory of Theoretical Physics, JINR, 141980 Dubna, Russia*
[2]*Departamento de Física Teórica—IFIC, Universidad de Valencia-CSIC, E-46100 Burjassot (Valencia), Spain*
[3]*Institut für Theoretische Physik II, Ruhr-Universität Bochum, D-44780 Bochum, Germany*

We perform a comparative theoretical study of the data at spacelike momentum transfer for the $\gamma^*\gamma \to \pi^0$ transition form factor, just reported by the Belle Collaboration, vs. those published before by *BABAR*, also including the older CLEO and CELLO data. Various implications for the structure of the π^0 distribution amplitude *vis-à-vis* those data are discussed and the existing theoretical predictions are classified into three distinct categories. We argue that the actual bifurcation of the data with antithetic trends is artificial and reason that the Belle data are the better option.

The newly released data for the pion-photon transition form factor (TFF) $F^{\gamma^*\gamma\pi^0}(Q^2, q^2 \to 0)$ by the Belle Collaboration [1], seem to be dramatically different from those reported in 2009 by the *BABAR* Collaboration [2]. Instead of a pronounced growth of the scaled TFF with Q^2, observed by *BABAR* above 9 GeV^2, the Belle data are compatible (with the exception of one point) at high Q^2 with the limit set by perturbative QCD [3]: $Q^2 F^{\gamma^*\gamma\pi^0} = \sqrt{2}f_\pi \approx 0.185$ GeV with $f_\pi = 131$ MeV.

The behavior of the π^0 TFF with increasing Q^2 can be forecast within calculable theoretical errors using the theoretical tools of QCD—perturbative and nonperturbative. Perturbative QCD governs evolution and supplies the means to calculate radiative corrections, whereas nonperturbative QCD provides the modeling concepts and techniques to determine the π^0 distribution amplitude (DA)—in leading-twist two and higher twists—and treat the hadronic structure of the nearly on-mass-shell photon.

In a recent paper [4], we have discussed what one should expect for the outcome of a measurement of the π^0 TFF at high Q^2 according to QCD. We argued that the expected scaling behavior should follow—within uncertainties—the interpolation formula of Brodsky and Lepage [5]: $F^{\gamma^*\gamma\pi}(Q^2) = (\sqrt{2}f_\pi)/(4\pi^2 f_\pi^2 + Q^2)$. This phenomenological formula links the TFF at $Q^2 = 0$, fixed by the axial anomaly, with the QCD asymptotic limit $\sqrt{2}f_\pi$. While plausible and useful in practical terms, this formula is not derived from QCD. Hence, it is of paramount importance to calculate the TFF within QCD in order to obtain an expression that can replicate the appearance of stasis in the scaled TFF above some Q^2 value as a result of switching on parton-photon interactions controlled by QCD. Such a saturating behavior of the TFF can be obtained from a formalism developed in a series of papers

[6–10] that combines the dispersive approach of light-cone sum rules (LCSRs) [11,12] (see also [13,14]) with QCD sum rules that employ nonlocal condensates [15,16]. The latter scheme is used to derive the pion DA, while the former serves to properly accommodate the hadronic content of the low-virtuality photon. Then, the TFF is defined by the LCSR

$$Q^2 F^{\gamma^*\gamma\pi}(Q^2) = \frac{\sqrt{2}}{3} f_\pi \left[\frac{Q^2}{m_\rho^2} \int_{x_0}^1 \exp\left(\frac{m_\rho^2 - Q^2 \bar{x}/x}{M^2} \right) \right.$$
$$\left. \times \bar{\rho}(Q^2, x) \frac{dx}{x} + \int_0^{x_0} \bar{\rho}(Q^2, x) \frac{dx}{\bar{x}} \right], \quad (1)$$

where the spectral density is given by $\bar{\rho}(Q^2, x) = (Q^2 + s)\rho^{\text{pert}}(Q^2, s)$ with $\rho^{\text{pert}}(Q^2, s) = (1/\pi)\text{Im}F^{\gamma^*\gamma^*\pi}(Q^2, -s - i\varepsilon)$, and the abbreviations $\bar{x} = 1 - x$, $s = \bar{x}Q^2/x$, $x_0 = Q^2/(Q^2 + s_0)$ have been used. The hadronic content of the quasireal photon in the TFF is taken care of by means of the first term in Eq. (1), whereas the partonic pointlike interactions above $s > s_0$ are described by the second term which is calculable order by order in QCD perturbation theory. Our computation is performed at the level of the NLO spectral density by taking into account the correction pointed out in [14]. The other parameters have the following values [7]: $s_0 = 1.5$ GeV^2, $m_\rho = 0.77$ GeV, while the Borel parameter is $M^2 = M_{2-\text{pt}}^2/\langle x \rangle_{Q^2} < 1$ GeV^2 from the two-point QCD sum rule for the ρ-meson with $M_{2-\text{pt}}^2 \in [0.5 \div 0.8]$ GeV^2 (see [10] for more details).

The twist-two pion DA in the formalism of Bakulev, Mikhailov, and Stefanis (BMS) [6] is modeled in terms of two Gegenbauer coefficients a_2 and a_4: $\varphi_\pi^{(2)\text{BMS}}(x) = \varphi^{\text{asy}}(x)[1 + a_2 C_2^{3/2}(2x - 1) + a_4 C_2^{3/2}(2x - 1)]$, where $\varphi^{\text{asy}}(x) = 6x\bar{x}$ denotes the asymptotic (asy) π^0 DA. The values of $a_2(\mu^2) = 0.20$ and $a_4(\mu^2) = -0.14$ (at $\mu^2 = 1$ GeV^2) are selected in such a way that the first ten moments $\langle \xi^N \rangle_\pi \equiv \int_0^1 dx (2x - 1)^N \varphi_\pi^{(2)}(x, \mu^2)$ with the normalization condition $\int_0^1 dx \varphi_\pi^{(2)}(x, \mu^2) = 1$ lie inside a particular range determined in [6], while all higher

*bakulev@theor.jinr.ru
†mikhs@theor.jinr.ru
‡alexandr.pimikov@uv.es
§stefanis@tp2.ruhr-uni-bochum.de

coefficients a_6, a_8, a_{10} were determined and found to be negligible. This procedure gives rise to a whole "bunch" of possible DAs whose shape is characterized by a double-humped structure with strongly suppressed endpoints $x = 0$, 1. This suppression is controlled by the vacuum quark virtuality $\lambda_q^2(\mu^2 = 1 \text{ GeV}^2) \approx 0.4 \text{ GeV}^2$ which characterizes the nonlocality of the quark (quark-gluon) condensate [6] and corresponds to a correlation length of about 0.31 fm. This parameter turns out to be intimately related to the Twist-four coupling $\delta^2(\mu^2)$ which has a value around $\delta^2 \approx \lambda_q^2/2$—details can be found in [7]. The *BABAR* data from $Q^2 = 10 \text{ GeV}^2$ onward show a marked tendency to increase with Q^2 and are therefore incompatible with the BMS formalism. These data can be best reproduced with a flat-top π^0 DA [17–19] that yields an auxetic TFF [4]—more below.

Let us look more closely in Fig. 1 at what the experimental data from different collaborations CELLO [20], CLEO [21], *BABAR* [2], and Belle [1] mean, comparing them with the results of several theoretical approaches. The shaded (green) band shows the predictions calculated using the BMS formalism detailed in [10]. The result for the BMS model [6] is represented by the solid line inside it, while the width of the band collects uncertainties from different sources: (i) the variation of the shape of the π^0 DA extracted from QCD sum rules with nonlocal condensates [6], (ii) the uncertainty of the Twist-four coupling δ^2 [7], and (iii) the sum of the Twist-six term [14] and the next-to-next-to-leading order (NNLO) radiative correction, proportional to the β_0 function, computed in [22]. The combined treatment of these last two uncertainties is justified because for the Borel parameter $M^2 \leq 1 \text{ GeV}^2$, we are adopting, see, e.g., [12], both have rather small magnitudes comparable in size but opposite signs, with the Twist-six term being positive.
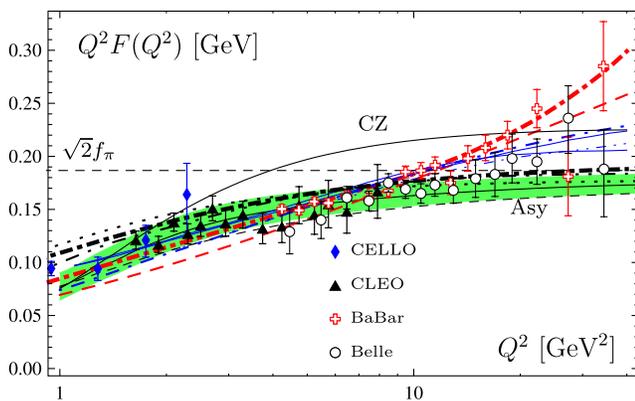
FIG. 1 (color online). Theoretical predictions for the scaled $\gamma^*\gamma\pi^0$ TFF, calculated in various approaches, in comparison with all existing experimental data, using for the latter the indicated notations. The shaded (green) band contains the results obtained within the BMS formalism in [10], with the solid line inside it denoting the prediction for the BMS model DA [6]. The other curves are explained in the text.

Dropping extraneous details, let us address the other curves shown in this figure from bottom to top. The dashed line at the lower border of the shaded (green) band—tagged Asy—denotes the TFF computed with the asymptotic π^0 DA. Next, the dotted [23] and the double-dotted-dashed [24] lines, partly intersecting with the band, give the results obtained with two holographic models based on the AdS/CFT correspondence. The thick dashed-dotted line at the upper boundary of the shaded band shows the recent prediction for the TFF obtained in [25] using an extended vector-dominance model. The intermediary (blue) solid lines denote the TFF obtained for models III (lower curve) and I (higher curve) from the LCSR analysis in [14], whereas the prediction of their model II lies in between (not shown). The key characteristic of these models for the π^0 DA is the large size of the coefficient $a_4 > a_2$ and the non-negligible values of the higher Gegenbauer coefficients a_6, a_8, a_{10}, a_{12}. Actually, model I is a flat-top DA with a reduced coefficient $a_2^{\text{flat-top}}(\mu^2 = 1 \text{ GeV}^2) \rightarrow$ 0.130, while model III has the coefficients $a_2 = 0.160$, $a_4 = 0.220$, $a_6 = 0.080$ (all values at 1 GeV^2) [14]—neglecting higher ones. Note that this analysis takes into account the twist-six contribution—found to be positive and very small for the adopted value of the Borel parameter $M^2 = 1.5 \text{ GeV}^2$, while it ignores the explicit inclusion of the (negative) NNLO radiative correction. As one sees from this figure, the inverse hierarchy of the Gegenbauer coefficients $a_2 < a_4$ in the LCSR approach of [14] turns out to be not really enough to fully account for the auxetic behavior of the *BABAR* data above 9 GeV^2, while for the same reason it causes a deviation from the Belle data and the asymptotic QCD limit.

A similar result—shown as a double-dotted-dashed (blue) line (Fig. 1) in the vicinity of the previous two curves—was obtained by Kroll in [26] using a different theoretical framework based on the Botts-Li-Sterman modified factorization scheme [27,28]. At the upper end of this regime of predictions one finds the TFF (long-dashed-dotted line), computed by Polyakov in [19] by using a flatlike π^0 DA, that was extracted from an effective chiral quark model based on the instanton vacuum of QCD and including leading-order (LO) evolution effects. The two (red) curves shown at the top represent the predictions obtained with a constant flat-top DA by Radyushkin [18] (dashed line) and Lih and Geng [29] (thick dashed-dotted line). For completion, also the prediction for the TFF for the Chernyak-Zhitnitsky (CZ) π^0 DA [30] is shown (solitary line with the CZ label).

The main message from Fig. 1 is that only with a flat-top pion DA one can really replicate the auxetic behavior of the $\pi^0 \rightarrow \gamma^*\gamma$ transition form factor exhibited by the high-Q^2 *BABAR* data [17–19]. It is worth noting, however, that to get best agreement in the statistical sense, one has to "cull" the two outliers at 14 and 27 GeV^2 before analysis. These two outliers are close to the asymptotic QCD limit

and hence, strictly speaking, incompatible with a flat-top π^0 DA. From the theoretical point of view, a flat-top DA reflects a contingency approach geared in hindsight with the only aim to emulate the auxetic trend of the *BABAR* data for the pion TFF. There are no features in some region of the longitudinal momentum fraction x of the valence quark and no humps anywhere. Of course, this scaling must eventually break down at the endpoints $x = 0$ and $x = 1$ because no parton can carry a larger momentum fraction than 1. Therefore, a flat-top π^0 DA describes the pion as being a "pointlike" particle with no internal structure because it looks the same everywhere [31]. On the other hand, the BMS formalism yields predictions that are possible only if the π^0 TFF is governed by QCD—in lingo: collinear factorization underlying Eq. (1). Accordingly, the TFF saturates at high momentum values of Q^2, meaning that the high-virtuality photon couples to a single parton inside the considered meson which is well-described by a BMS-like DA that incorporates the nonlocality of the QCD vacuum. In contrast, the *BABAR* data [2] for the pion contradict this behavior necessitating some nonperturbative mechanism capable of providing, e.g., $\ln(Q^2/\mu^2)$ enhancement (where μ^2 is some contextual nonperturbative scale <1 GeV^2) to the TFF, as encoded in a flat-top π^0 DA [17–19]. In short, the invention of a flatlike DA within a specific context is contingent on the unforeseen behavior of the π^0 *BABAR* data at high Q^2. Would the outcome of these data be in line with the asymptotic QCD prediction, attempts to create a flatlike π^0 DA to challenge the collinear QCD factorization would appear contrived and artificial. Relying instead solely on the Belle data [1], there would be no need at all to invoke a flatlike DA based explanation of the π^0 TFF.

The dichotomy between scaling of the TFF with Q^2 and auxesis becomes more evident by inspecting Fig. 2 which summarizes the experimental situation for the π^0 TFF in conjunction with the predictions of various theoretical approaches. The latter can be organized into three distinct shaded bands, whose widths are adjusted to include similar predictions obtained in different theoretical schemes and are not related to particular inherent theoretical uncertainties (like the BMS band shown in Fig. 1). The main goal of presenting Fig. 2 is to place the π^0 TFF in a broader perspective by collecting and comparing what is known experimentally and categorizing what has been proposed theoretically. The central observation is that the experimental data for the π^0 TFF arrange themselves at high-Q^2 values (starting at 10 GeV^2) along two branches which below this value unify into a single one. The upper branch of the data consists only of the *BABAR* data for the π^0 TFF [2]—with the exception of the two outliers downwards at 14 and 27 GeV^2, already mentioned in the discussion of Fig. 1, and the Belle outlier upwards at $Q^2 = 27.33$ GeV^2. The lower branch contains the two *BABAR* outliers and all the other Belle data. One can also count to this branch the
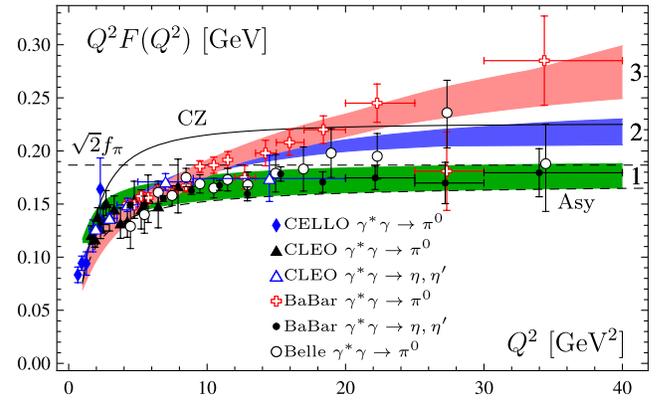
FIG. 2 (color online). Classification of theoretical predictions for the spacelike scaled TFFs of the π^0 and the nonstrange component $|n\rangle$ of the η, and η' in terms of three distinct shaded bands in comparison with all existing experimental data with notations as indicated. The predictions for the asymptotic (lowest dashed line) and the CZ DAs (solid line) are explicitly labeled.

data for $(3/5)Q^2 F^{\gamma^*\gamma n}$, where $|n\rangle = (1/2)(|u\bar{u}\rangle + |d\bar{d}\rangle)$, extracted from the *BABAR* data [32] for η and η'—see [4] for more.

The classification of the theoretical predictions follows roughly this pattern plus an additional band in between. Those predictions agreeing with the standard QCD factorization scheme are forming the lower (dark-green) band, labeled 1. To be specific, this band contains the predictions obtained within the BMS formalism in our most recent analysis in [10,33–35], where one can find the details. Moreover, band 1 includes the result of the form-factor modeling of [25], based on an extended vector-dominance model. Interestingly, also the predictions from two different AdS/QCD models, viz., [23,24,36], lie within band 1. The lower boundary of this band is compatible with the asymptotic π^0 DA (dashed line with the flag Asy).

The (red) band 3 collects the results from [18,29], which both employ a flat-top π^0 DA, as well as that of the analysis in [37] which utilizes a flatlike DA and Sudakov effects. The predictions from [38–40], based on a dispersive representation of the axial anomaly and quark-hadron duality, are within this band as well. The similar results of [41] are also incorporated, while the findings of [42,43] (not shown) would appear just below the edge of band 3. Moreover, band 3 contains the result of the calculation in [44] which ascribes the auxetic TFF behavior to new physics in the τ sector.

Between the two aforementioned bands, one has another class of theoretical predictions forming the (blue) band 2. This consists of the results obtained with models I, II, and III of the LCSR analysis of [14], Polyakov's result [19], extracted from the chiral quark model, and also an analogous result from [45]. Note that the curve representing the TFF computed with the CZ DA (shown as a single solid line with the label CZ) joins band 2 at the far end of the experimentally accessible momentum region, while it is

TABLE I. We show in the first row the $\chi^2/$ndf for the BMS model [6] in comparison with estimates of the coefficients a_n of the π DA determined by fitting the pion-photon TFF within LCSRs. The second and third rows show a 2D fit in the (a_2, a_4) plane, while the last two rows employ a nonzero coefficient a_6. The errors are due to statistical uncertainties and a systematic error related to the Twist-four term. The last column shows the values of $\chi^2/$ndf (with ndf = number of degrees of freedom) for the considered data sets. (All entries evaluated at $\mu_{SY}^2 = 5.76$ GeV^2 with SY abbreviating Schmedding and Yakovlev [13]).

Data set	$a_2(\mu_{SY}^2)$	$a_4(\mu_{SY}^2)$	$a_6(\mu_{SY}^2)$	$\chi^2/$ndf
CELLO [20], CLEO [21], Belle [1]	0.142	−0.090	0	22.1/33
CELLO, CLEO, Belle	$0.154 \pm 0.046 \pm 0.055$	$-0.066 \pm 0.067 \pm 0.058$	0	20.1/31
CELLO, CLEO, *BABAR* [2]	$0.090 \pm 0.037 \pm 0.050$	$0.069 \pm 0.057 \pm 0.053$	0	69.5/33
CELLO, CLEO, Belle	$0.157 \pm 0.057 \pm 0.056$	$-0.192 \pm 0.122 \pm 0.077$	$0.226 \pm 0.161 \pm 0.033$	13.1/30
CELLO, CLEO, *BABAR*	$0.177 \pm 0.054 \pm 0.056$	$-0.171 \pm 0.103 \pm 0.071$	$0.307 \pm 0.096 \pm 0.024$	33.3/32

more than 4σ away from all data below 10 GeV^2. Except the calculations giving rise to strip 3, most other predictions shown in Fig. 2 include Efremov-Radyushkin-Brodsky-Lepage [46,47] evolution at the LO or NLO level.

In Table I, we present statistical fits of the pion TFF, calculated with LCSRs to the data. The first row shows the original BMS values from [6], while the next two rows show a 2D fit to two sets of data using only the first two coefficients a_2 and a_4. One set contains the CELLO, CLEO, and Belle data, while the other one consists of the CELLO, CLEO, and *BABAR* data. The last two rows represent an analogous fit which also employs the next coefficient a_6. Evidently, the Belle data allow in both cases a better statistical description. This distinct behavior completely agrees with our classification scheme presented in Fig. 2, with the BMS model and the 2D best-fit being entirely inside band 1.

But from another more data-oriented point of view, one may argue (see, e.g., [48]) that one should not distinguish the data as we did in Fig. 2 because the relative deviation between the Belle and the *BABAR* fits does not exceed 1.5σ [1]. Appealing to this comparability, one may be tempted to unify the theoretical results, shown in terms of three distinct strips in the previous figure, into a single wide band. This is illustrated in Fig. 3, where the darker shading of the band toward the top indicates the deviation from scaling with Q^2 predicted by QCD towards an auxetic TFF behavior contingent on model-dependent explanations. Thus, even if such data pooling seems statistically acceptable, the underlying theoretical approaches are hardly comparable to each other, so that an interpretation of the Belle and the *BABAR* data in relation to each other and against some common standard appears rather questionable. In this figure, all data sets are represented by single fits as follows: (i) The top solid line shows a power-law fit $Q^2|F(Q^2)| = A(Q^2/10 \text{ GeV}^2)^\beta$ to the *BABAR* data with $A = 0.182$, $\beta = 0.25$ [2]. (ii) The lower (blue) solid line is also a power-law fit to the Belle data with $A = 0.169$ GeV, $\beta = 0.18$ [1], whereas the dashed (blue) line below denotes a dipole fit $Q^2|F(Q^2)| = BQ^2/(Q^2 + C)$ to the Belle data with $B = 0.209$ GeV, $C = 2.2$ GeV^2 [1]. (iii) The thick dashed line at the bottom shows the dipole fit to the CLEO data [21] with $B = 0.171$ GeV, $C = 0.6$ GeV^2.

The appearance of the Belle data [1] on the π^0 TFF forces us to consider the two-photon processes of light pseudoscalar mesons in a greater perspective because the trend of these data shows an antithetic behavior relative to that reported by *BABAR* [2] with a relative deviation of about 1.5σ [1]. Instead of a pronounced rise with Q^2, it levels off and follows more or less the scaling behavior predicted by QCD and collinear factorization. Though this is welcome from the theoretical point of view, an increasing TFF behavior with Q^2 cannot be ruled out at present—at least as long as no possible sources of errors have been identified by the *BABAR* Collaboration to revoke the validity of their results. However, given that no unique QCD mechanism has been proposed to provide the necessary enhancement of the π^0 TFF in order to reconcile the *BABAR* data with QCD, it seems reasonable to consider the auxetic behavior of the *BABAR* data and the entailed discrepancy to QCD as an anomaly. This view is strengthened by the fact that the pivotal QCD effects, notably, the NLO and (the main) NNLO radiative corrections, Efremov-Radyushkin-Brodsky-Lepage evolution, and the Twist-four term give suppression to the TFF, except the Twist-six correction which is either small or of the same size as the NNLO term but with opposite sign, hence
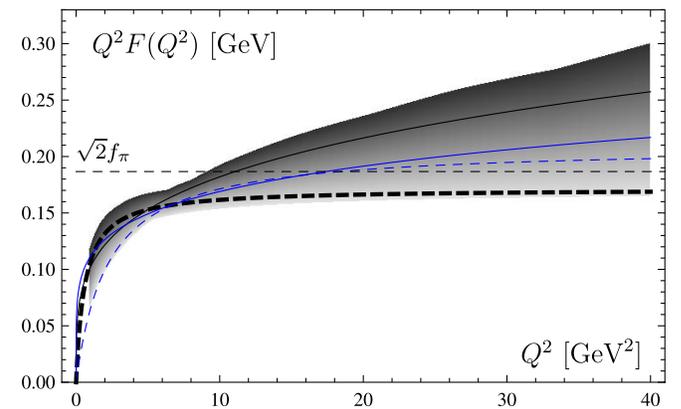
FIG. 3 (color online). Unified range of theoretical predictions (grey area) discussed in context with Fig. 2. The darker shading indicates transition from scaling with Q^2 to auxesis. The experimental data of CLEO, Belle, and *BABAR* are shown in terms of fits (single lines) explained in the text.

canceling against it. Moreover, including in the theoretical analysis a small but finite virtuality of the quasireal photon, as in real single-tagged experiments, also yields to suppression [4,25,49,50], albeit this suppression is more significant at lower Q^2 values.

The bottom line is that skepticism about the accuracy of the *BABAR* data at high Q^2 prevails, giving preference to the Belle results that found no deviation from the standard QCD scheme. Moreover, in that case there is no chasm between the TFFs of the π^0 and the $|n\rangle$, i.e., no evidence for a significant flavor-symmetry breaking in the pseudoscalar meson sector of QCD—in accordance with all previous experiments.

[1] S. Uehara *et al.*, arXiv:1205.3249.
[2] B. Aubert *et al.*, Phys. Rev. D **80**, 052002 (2009).
[3] S. J. Brodsky and G. P. Lepage, Phys. Rev. D **24**, 1808 (1981).
[4] N. G. Stefanis, A. P. Bakulev, S. V. Mikhailov, and A. V. Pimikov, arXiv:1202.1781.
[5] S. J. Brodsky and G. P. Lepage, Adv. Ser. Dir. High Energy Phys. **5**, 93 (1989).
[6] A. P. Bakulev, S. V. Mikhailov, and N. G. Stefanis, Phys. Lett. B **508**, 279 (2001); **590**, 309(E) (2004).
[7] A. P. Bakulev, S. V. Mikhailov, and N. G. Stefanis, Phys. Rev. D **67**, 074012 (2003).
[8] A. P. Bakulev, S. V. Mikhailov, and N. G. Stefanis, Phys. Lett. B **578**, 91 (2004); Phys. Rev. D **73**, 056002 (2006).
[9] S. V. Mikhailov and N. G. Stefanis, Nucl. Phys. **B821**, 291 (2009).
[10] A. P. Bakulev, S. V. Mikhailov, A. V. Pimikov, and N. G. Stefanis, Phys. Rev. D **84**, 034014 (2011).
[11] I. I. Balitsky, V. M. Braun, and A. V. Kolesnichenko, Nucl. Phys. **B312**, 509 (1989).
[12] A. Khodjamirian, Eur. Phys. J. C **6**, 477 (1999).
[13] A. Schmedding and O. Yakovlev, Phys. Rev. D **62**, 116002 (2000).
[14] S. S. Agaev, V. M. Braun, N. Offen, and F. A. Porkert, Phys. Rev. D **83**, 054020 (2011).
[15] S. V. Mikhailov and A. V. Radyushkin, JETP Lett. **43**, 712 (1986); Sov. J. Nucl. Phys. **49**, 494 (1989).
[16] A. P. Bakulev and A. V. Radyushkin, Phys. Lett. B **271**, 223 (1991).
[17] A. E. Dorokhov, Phys. Part. Nucl. Lett. **7**, 229 (2010).
[18] A. V. Radyushkin, Phys. Rev. D **80**, 094009 (2009).
[19] M. V. Polyakov, JETP Lett. **90**, 228 (2009).
[20] H. J. Behrend *et al.*, Z. Phys. C **49**, 401 (1991).
[21] J. Gronberg *et al.*, Phys. Rev. D **57**, 33 (1998).
[22] B. Melić, D. Müller, and K. Passek-Kumerički, Phys. Rev. D **68**, 014013 (2003).
[23] S. J. Brodsky, F.-G. Cao, and G. F. de Teramond, Phys. Rev. D **84**, 033001 (2011).
[24] H. R. Grigoryan and A. V. Radyushkin, Phys. Rev. D **78**, 115008 (2008).
[25] H. Czyż, S. Ivashyn, A. Korchin, and O. Shekhovtsova, Phys. Rev. D **85**, 094010 (2012).
[26] P. Kroll, Eur. Phys. J. C **71**, 1623 (2011).
[27] J. Botts and G. Sterman, Nucl. Phys. **B325**, 62 (1989).
[28] H.-n. Li and G. Sterman, Nucl. Phys. **B381**, 129 (1992).
[29] C.-C. Lih and C.-Q. Geng, Phys. Rev. C **85**, 018201 (2012).
[30] V. L. Chernyak and A. R. Zhitnitsky, Phys. Rep. **112**, 173 (1984).
[31] H. L. L. Roberts *et al.*, Phys. Rev. C **82**, 065202 (2010).
[32] P. del Amo Sanchez *et al.*, Phys. Rev. D **84**, 052001 (2011).
[33] A. P. Bakulev, S. V. Mikhailov, A. V. Pimikov, and N. G. Stefanis, Nucl. Phys. B, Proc. Suppl. **219–220**, 133 (2011).
[34] N. G. Stefanis, Few-Body Syst. **52**, 415 (2012).
[35] N. G. Stefanis, A. P. Bakulev, S. V. Mikhailov, and A. V. Pimikov, Nucl. Phys. B, Proc. Suppl. **225–227**, 146 (2012).
[36] S. J. Brodsky, F.-G. Cao, and G. F. de Teramond, Phys. Rev. D **84**, 075012 (2011).
[37] H.-n. Li and S. Mishima, Phys. Rev. D **80**, 074024 (2009).
[38] Y. N. Klopot, A. G. Oganesian, and O. V. Teryaev, Phys. Rev. D **84**, 051901 (2011).
[39] Y. N. Klopot, A. G. Oganesian, and O. V. Teryaev, Phys. Lett. B **695**, 130 (2011).
[40] D. Melikhov and B. Stech, Phys. Rev. D **85**, 051901 (2012).
[41] T. N. Pham and X. Y. Pham, Int. J. Mod. Phys. A **26**, 4125 (2011).
[42] X.-G. Wu and T. Huang, Phys. Rev. D **82**, 034024 (2010).
[43] X.-G. Wu and T. Huang, Phys. Rev. D **84**, 074011 (2011).
[44] D. McKeen, M. Pospelov, and J. M. Roney, Phys. Rev. D **85**, 053002 (2012).
[45] S. Noguera and V. Vento, Eur. Phys. J. A **46**, 197 (2010).
[46] A. V. Efremov and A. V. Radyushkin, Phys. Lett. **94B**, 245 (1980).
[47] G. P. Lepage and S. J. Brodsky, Phys. Rev. D **22**, 2157 (1980).
[48] S. Noguera and V. Vento, arXiv:1205.4598.
[49] E. R. Arriola and W. Broniowski, Phys. Rev. D **81**, 094021 (2010).
[50] P. Lichard, Phys. Rev. D **83**, 037503 (2011).